

Dr. 1476

350

SERI/TP-721-574
UC CATEGORY: UC-59

PERFORMANCE OF STORAGE WALLS WITH
HIGHLY CONDUCTIVE COVERING PLATES
AND CONNECTING FINS

JOSEPH K. E. ORTEGA
CARL E. BINGHAM
J. MICHAEL CONNOLLY

MAY 1980

MASTER

PREPARED UNDER TASK NO. 6321.10

Solar Energy Research Institute

1536 Cole Boulevard
Golden, Colorado 80401

A Division of Midwest Research Institute

Prepared for the
U.S. Department of Energy
Contract No. EG-77-C-01-4042

DISTRIBUTION OF THIS DOCUMENT IS UNLIMITED

DISCLAIMER

This report was prepared as an account of work sponsored by an agency of the United States Government. Neither the United States Government nor any agency Thereof, nor any of their employees, makes any warranty, express or implied, or assumes any legal liability or responsibility for the accuracy, completeness, or usefulness of any information, apparatus, product, or process disclosed, or represents that its use would not infringe privately owned rights. Reference herein to any specific commercial product, process, or service by trade name, trademark, manufacturer, or otherwise does not necessarily constitute or imply its endorsement, recommendation, or favoring by the United States Government or any agency thereof. The views and opinions of authors expressed herein do not necessarily state or reflect those of the United States Government or any agency thereof.

DISCLAIMER

Portions of this document may be illegible in electronic image products. Images are produced from the best available original document.

Printed in the United States of America
Available from:
National Technical Information Service
U.S. Department of Commerce
5285 Port Royal Road
Springfield, VA 22161
Price:

Microfiche \$3.00
Printed Copy \$ 4.00

NOTICE

This report was prepared as an account of work sponsored by the United States Government. Neither the United States nor the United States Department of Energy, nor any of their employees, nor any of their contractors, subcontractors, or their employees, makes any warranty, express or implied, or assumes any legal liability or responsibility for the accuracy, completeness or usefulness of any information, apparatus, product or process disclosed, or represents that its use would not infringe privately owned rights.

**PERFORMANCE OF STORAGE WALLS WITH
HIGHLY CONDUCTIVE COVERING PLATES AND CONNECTING FINS**

Joseph K. E. Ortega
Senior Research Engineer
Passive Technology Branch
Solar Energy Research Institute
Golden, Colorado
Assoc. Mem. ASME

Carl E. Bingham
Staff Engineer
Passive Technology Branch
Solar Energy Research Institute
Golden, Colorado

J. Michael Connolly
Senior Engineer
Passive Technology Branch
Solar Energy Research Institute
Golden, Colorado


ABSTRACT

The thermal behavior of a storage wall, constructed of concrete with highly conductive covering plates and connecting vertical fins, is investigated. The results demonstrate that, during the charging mode, the amount of energy released from the front surface is significantly reduced. A portion of the saved energy is stored for future discharge, but a large portion is transferred to the back surface and released. A selective front surface further reduces the energy released from the front surface, and this energy is stored. By properly selecting the fin spacing, plate-fin thickness, and plate-fin thermal conductivity, the rate and direction of thermal discharge can be controlled. The improved heat transfer capability and added thermal control provide new alternatives for interzonal heat transfer and multizone passive building designs.

DISCLAIMER

This book was prepared as an account of work sponsored by an agency of the United States Government. Neither the United States Government nor any agency thereof, nor any of their employees, makes any warranty, express or implied, or assumes any legal liability or responsibility for the accuracy, completeness, or usefulness of any information, apparatus, product, or process disclosed, or represents that its use would not infringe privately owned rights. Reference herein to any specific commercial product, process, or service by trade name, trademark, manufacturer, or otherwise, does not necessarily constitute or imply its endorsement, recommendation, or favoring by the United States Government or any agency thereof. The views and opinions of authors expressed herein do not necessarily state or reflect those of the United States Government or any agency thereof.

DISTRIBUTION OF THIS DOCUMENT IS UNLIMITED.

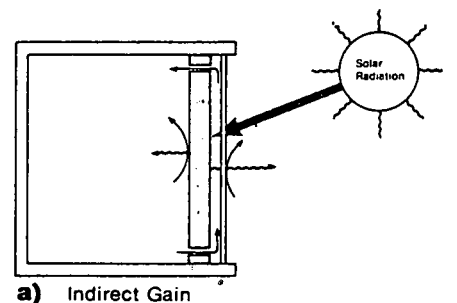


1. INTRODUCTION

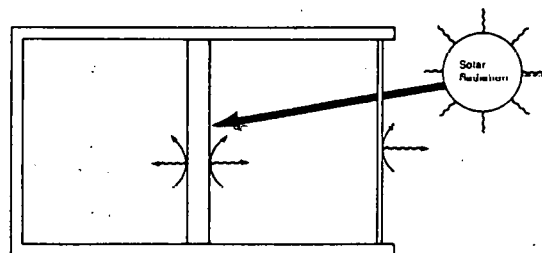
The thermal storage wall is a fundamental element of many passive solar building designs. The material used in storage walls is most commonly either masonry or water. Normally the storage wall is strategically located to absorb solar radiation during the day (charging mode) and release thermal energy to the building interior, via thermal radiation and free convection, at night (discharging mode). Frequently, it is advantageous to reduce the energy released from the front (south) surface of the storage wall during charging. This is especially true for direct and indirect gain passive designs (Figure 1). In indirect gain passive designs, some of the energy released from the front surface is lost through the glazing. In the direct gain system, thermal energy released during the day from the front surface is usually unwelcome, because the comfort level depends on air temperature, mean radiant temperature, and solar radiation; an increase in solar radiation and/or mean radiant temperature requires a decrease in air temperature to maintain the same comfort level.

The present study investigates the thermal behavior of a transfer wall constructed of concrete with highly conductive covering plates and connecting vertical fins to determine if such a wall can provide thermal control and improve thermal performance.

The results demonstrate that this type of construction can significantly reduce energy losses from the front surface during charging. A portion of this saved energy is stored for future discharge, but a larger portion is transferred to the back wall surface and released (to the interior or north zone). This improved heat transfer capability provides new alternatives for interzonal heat transfer and multizone passive building designs.



a) Indirect Gain



b) Direct Gain - Two Zones

Fig. 1. Indirect and direct gain passive designs.

The effect of a selective radiation coating on the front surface of this transfer wall was also investigated. The results demonstrate that a selective radiation coating further reduces front losses, increases stored energy for future discharge, and increases the amount of energy transferred to the back surface. By properly selecting the spacing between connecting fins, fin thickness, plate-fin thermal conductivity and using selective coatings, a significant amount of control over the amount of energy stored and the direction of thermal discharge can be obtained.

2. DESCRIPTION AND METHOD

The thermal behavior of the transfer wall was investigated during charging and discharging modes and compared to that of a conventional homogenous isotropic concrete storage wall. The transfer wall investigated (Figure 2a) was constructed of concrete ($k = 1.315 \text{ W m}^{-1} \text{ }^\circ\text{C}^{-1}$) sandwiched between two highly conductive aluminum plates ($k = 192 \text{ W m}^{-1} \text{ }^\circ\text{C}^{-1}$). The plates were connected by vertical aluminum fins that ran the height of the storage wall. The thickness of the aluminum covering plates and connecting fins varied (2.54, 1.27, and 0.635 cm, or 1.0, 0.5, and 0.25 in, respectively). The thickness of the concrete was 0.305 m (1.0 ft). The spacing between connecting fins varied (0.152, 0.305, 0.61, and 1.22 m, or 0.5, 1.0, 2.0, and 4.0 ft, respectively).

The transfer wall and conventional concrete storage wall were investigated using the numerical simulation program MITAS (1,2). MITAS is a generalized, three-dimensional, heat transfer computer program using finite differencing techniques (forward, backward, and forward-backward) to obtain a transient solution for node temperatures and heat flows between nodes of a representative thermal nodal network. (Figure 2b shows part of the 66-node thermal model used to investigate the behavior of symmetric representative sections of the transfer and conventional storage wall. The 66 nodes consisted of 64 diffusion nodes to model the concrete portion of the wall, the aluminum cover plate and connecting fins, and two constant-temperature sink nodes.)

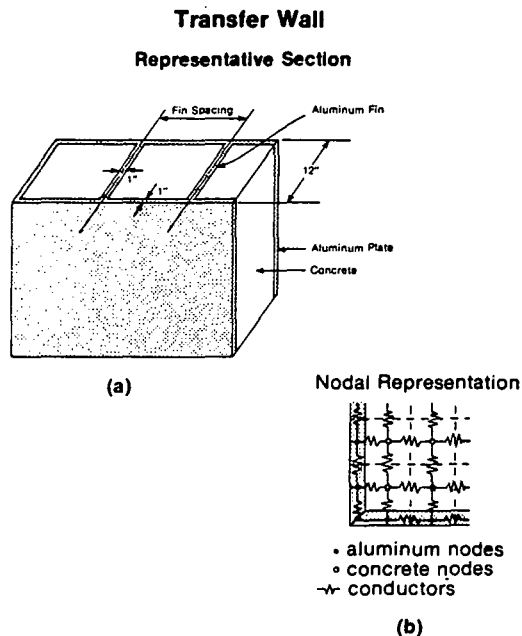


Fig. 2. A representative section of the transfer wall (a) and a portion of the nodal representation of the two-dimensional cross section investigated (b).

A two-dimensional model of a symmetric representative section was used because the thermal properties of the transfer wall do not vary with height, and a constant, uniform incident solar flux is simulated during charging. Furthermore, energy exchange with the surroundings is restricted to the front and back wall surfaces, where the model releases energy to a sink node held at $21.1 \text{ }^\circ\text{C}$ (70°F), the temperature of the storage wall before charging. Constant incident solar

flux and constant sink-node temperatures were used so that the resulting transient thermal behavior of the storage wall could more easily be characterized using nondimensional parameters. A later investigation will address the performance of the transfer wall with time-varying boundary conditions and incident solar flux. The uniform irradiation assumption on storage walls with and without highly conductive covering plates is shown to result in a small and insignificant error in the thermal performance of the storage wall (2).

Two forms of heat transfer from surface to sink were simulated: thermal radiation and free convection. The radiation losses from a nonselective and a selective surface were simulated using respective values for the emissivity of the surface: $\epsilon = 0.8$ (nonselective) and $\epsilon = 0.2$ (selective). The MITAS solution technique solves a quartic equation, thus eliminating the need to linearize the radiation conductors. Natural convection conductors from the surfaces to the sink node were temperature dependent and updated every time-step. Empirical relationships between the Nusselt and Rayleigh numbers (3) were used to derive the temperature-dependent film coefficient for free convection along the vertical surfaces.

Storage wall charging was simulated by applying a constant heat flux of 631 W m^{-2} ($200 \text{ Btu h}^{-1} \text{ ft}^{-2}$) for 6 h to the front surface. Then the storage wall discharged for 18 h. The temperature of each node and the energy exchange between nodes were calculated every 0.001 h.

3. RESULTS

3.1 Charging (Varying Fin Spacing)

Figure 3 presents the thermal performance of five storage walls during six hours of charging; four are transfer walls with different fin spacings, and the fifth (control) is a conventional concrete wall. The thickness of the covering plate and connecting fins are 2.54 cm (1 in). Figure 3a plots the sum of the energy stored and energy released from the back surface of the wall (energy gain) normalized by the incident radiation versus time. Each point in Fig. 3 represents the integrated value over that two-hour interval. Each curve represents the performance of one transfer wall with a given aspect ratio (the distance between fins divided by the thickness of the wall). Figure 3a can also be interpreted as the difference between energy absorbed and energy released by the front surface. All the transfer walls reduce the amount of thermal energy released from the front surface, and these losses become smaller with decreasing aspect ratios. At the end of a six-hour charging period, the normalized energy gain can be improved by as much as 22% of the incident energy by using a transfer wall with an aspect ratio of 0.5.

Some of this saved energy is stored. Figure 3b is a plot of the normalized stored energy versus time. As the aspect ratio decreases, more incident energy is stored. This finding is demonstrated in another way in Figure 3c, which shows that the sum of the normalized energy released from the front and back surfaces decreases with decreasing aspect ratio. In general, about half of the saved energy (the difference in gain between the transfer wall and conventional wall) is stored, and the amount varies with aspect ratio. The rest of the energy is released at the back surface. Figure 3d shows the improved heat transfer by plotting the ratio of energy released at the back surface to front surface, versus time. The improvement is dramatic. Fin spacings as large as four feet can increase the energy release ratio more than ten times that of a conventional storage wall over a six-hour charging period. As the aspect ratio decreases, the heat transfer rates increase.

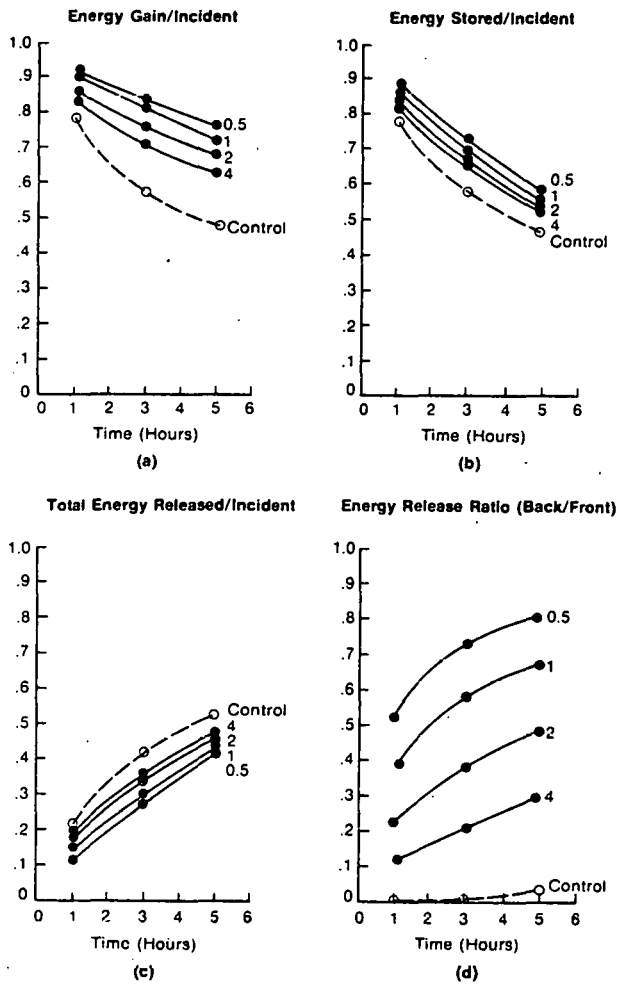


Fig. 3. Energy stored and released during the charging period, normalized to the incident radiation (1262 W h m^{-2} or 400 Btu ft^{-2}) during two-hour time intervals. Each point is an integrated value over the two-hour interval. Values for the aspect ratios (4, 2, 1, and 0.5) are plotted along with values for the conventional concrete storage wall (control).

3.2 Discharging (Varying Pin Spacing)

Figure 4 presents the thermal behavior of the same five storage walls during 18 h of discharging. Figure 4a is a plot of the energy release ratio, back to front, versus time. Each point represents an integrated value over a 4-hour interval, except for the first point, which is integrated over a 2-hour interval. A conventional storage wall releases most of its stored energy from its front surface. The transfer walls release more energy from the back than conventional walls, and within hours energy released from back and front surfaces are equal. As the aspect ratio decreases, equality of back and front losses is achieved faster. An increase in energy released from the back surface is almost always advantageous if the volume to be heated is enclosed by the back surface of the storage wall, i.e., the indirect gain passive designs. Also, this behavior is advantageous in a two-zone passive design (where the storage wall divides the two zones to be heated). In this case, heat is discharged equally to both rooms, eliminating the need to use fans, or other mechanical devices, to distribute the heat.

Figure 4b plots the total energy stored, normalized by the total incident energy absorbed during charging, versus time. These are instantaneous values. The differing initial values reflect the relative effective capacities of the walls (charging conditions and thermal capacitance are identical).

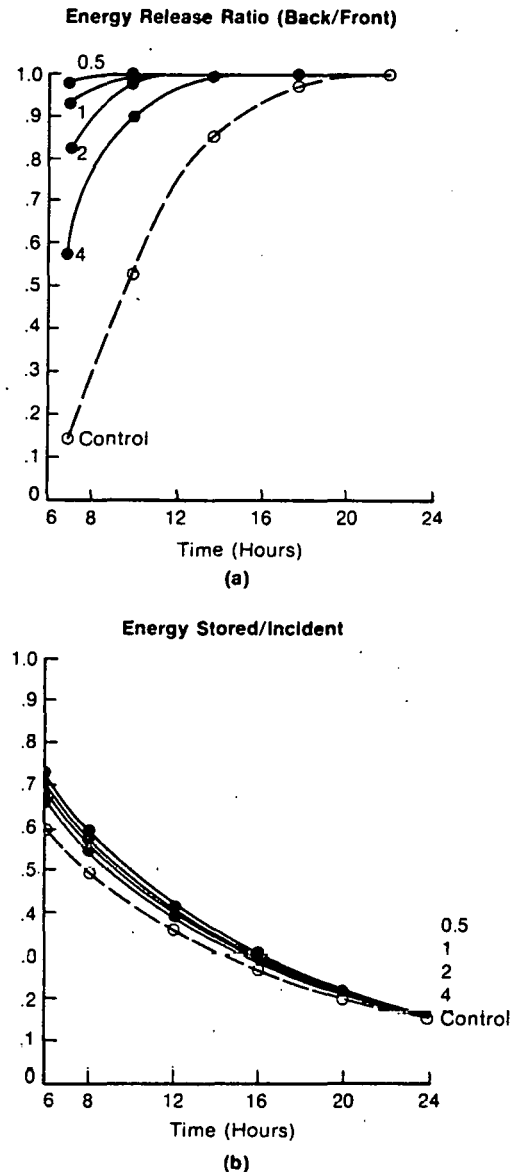


Fig. 4. In the top figure (a), each point is the ratio of energy released from the back to front surfaces over a four-hour interval, with the exception of the first point, which is for a two-hour period. In the bottom figure (b), instantaneous storage values per total incident radiation (3785 W h m^{-2} or 1200 Btu ft^{-2}) are plotted against time.

All the transfer walls store more energy after charging than a conventional wall. For large aspect ratios (2 and 4), the increase is small. Larger increases are obtained with smaller aspect ratios. The rate of energy discharge for all transfer walls is increased.

3.3 Varying Plate and Fin Thickness

The effect of different fin thicknesses on the performance of the transfer wall was investigated. The resulting thermal behavior is presented in Figures 5 and 6. The same charging and discharging scenario (6 h and 18 h, respectively) was used. Also, a constant aspect ratio of one was used for all of the simulations presented in Figures 5 and 6.

Charging. Figure 5 presents the thermal performance of the transfer wall with three different thicknesses for the aluminum cover plate and connecting fins: 2.54, 1.27, and 0.635 cm (1.0, 0.5, and 0.25 in, respectively). The results are similar to those results of the transfer walls with varying aspect ratios (Figure 3). For all plate-fin thicknesses, the transfer wall increases the normalized energy gain, normalized stored energy, and the energy release ratio (back/front) over that of a conventional storage. This increase is large for larger plate-fin thicknesses, as expected. Also as expected, the energy lost from the front surface decreases as the plate-fin thickness increases.

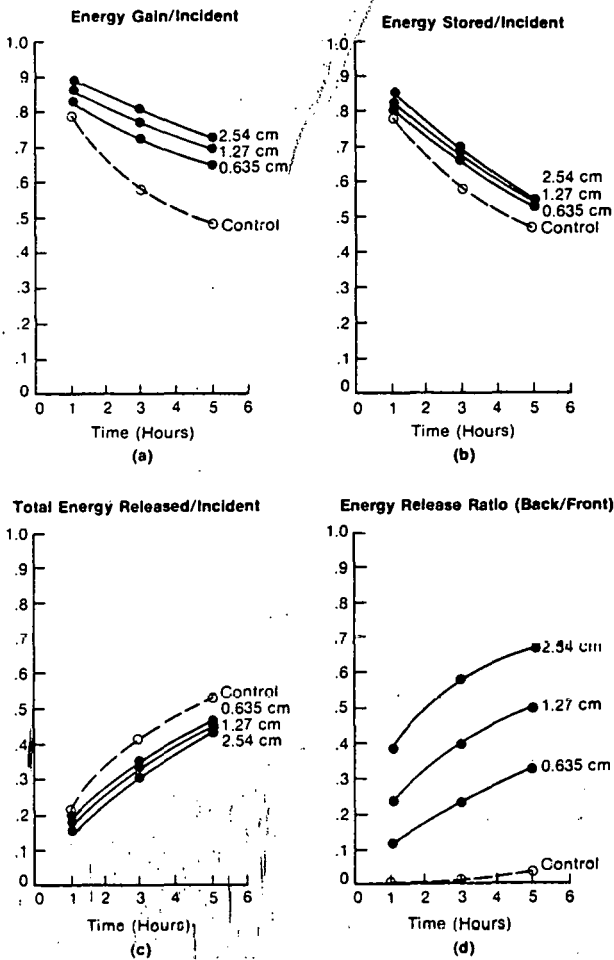


Fig. 5. Energy stored and released during the charging period. Same as Fig. 3, except values plotted are for fin thicknesses of 2.54, 1.27, and 0.635 cm (1.0, 0.5, 0.25 in, respectively) with an aspect ratio of 1.

Discharging. Figure 6 presents the thermal performance of the same four storage walls presented in Figure 5 during 18 h of discharging. Again, the results are similar to those results of the transfer walls with varying aspect ratios (Figure 4). For all plate and fin thickness, the transfer walls improve the amount of energy released from the back surface when compared to a conventional storage wall, Figure 6a. With a plate and fin thickness of only 0.635 cm (0.25 in) the energy released from back and front surfaces are equal within 8 h. As the plate-fin thicknesses increase, equality of back and front losses is achieved faster.

As before, the rate of energy discharge is improved with the transfer walls, Figure 6b.

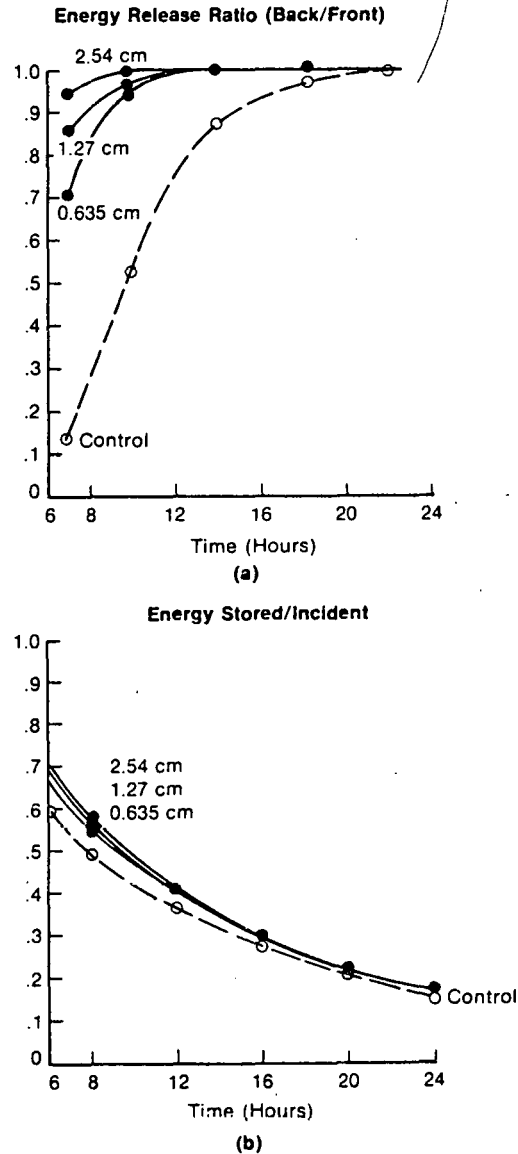


Fig. 6. Energy stored and released during the discharging period. Same as Fig. 4, except values plotted are for fin thicknesses of 2.54, 1.27, and 0.635 cm (1.0, 0.5, 0.25 in, respectively) with an aspect ratio of 1.

Total Conductance. The similar thermal behavior demonstrated by transfer walls with varying aspect ratios, and varying plate-fin thicknesses, suggests that a single thermal parameter can be used to obtain the effect of either varying aspect ratio or plate-fin thickness. Figures 7 and 8 demonstrate the thermal performance of the transfer wall with varying aspect ratio (solid dots) and varying plate-fin thicknesses (squares) when plotted against the total surface-to-surface conductance, K/L . In Figure 7 (charging) and Figure 8 (discharging), each point is an integrated value over the entire charging period (6 h) and discharging period (6-24 h), respectively, normalized to the total incident energy (3785 Wh m^{-2} , or 1200 Btu ft^{-2}).

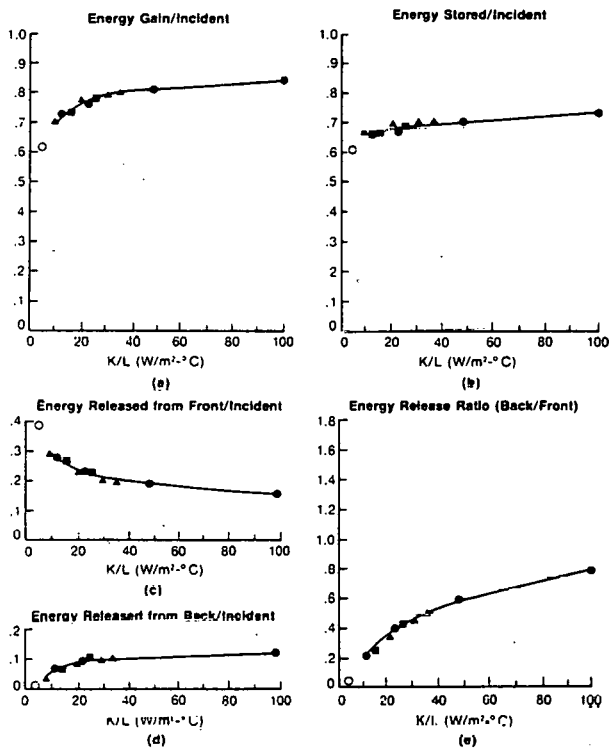


Fig. 7. The effect of aspect ratio and fin thickness during charging. K/L is the sum of the conductances of the concrete and the aluminum fins from the front to the back surface normalized to one square meter of storage wall surface. Aspect ratios (solid dots) of 4, 2, 1, and 0.5 (representing K/L equal to 11.62, 22.45, 46.73, and 97.63 $\text{W m}^{-2} \text{ } ^\circ\text{C}^{-1}$, respectively), and fin thicknesses (squares) of 2.54, 1.27, and 0.635 cm (representing K/L equal to 46.73, 25.50, and 14.90 $\text{W m}^{-2} \text{ } ^\circ\text{C}^{-1}$, respectively with an aspect ratio of 1) are shown, along with values for a conventional concrete storage wall (open circle, $K/L = 4.31 \text{ W m}^{-2} \text{ } ^\circ\text{C}^{-1}$). Also shown are results of various fin-plate thermal conductivities (triangles). Plate-fin materials used were stainless steel, iron, hydronalium, and silumin-copper with K/L values of 8.84, 20.62, 29.33, and 34.64 respectively. All values are integrated over the 6-hour charging period.

The conductance parameter K/L is defined as the total conduction coupling from the front to the back through a wall segment ($\text{W } ^\circ\text{C}^{-1}$) divided by the front face area (m^2). The total conduction coupling from the front to the back includes conduction through the covering plate and fins as well as the concrete core material. The conduction path length through

the concrete core material is equal to the wall thickness. However, the path length through the fin was increased by one-fourth the cover plate length. This additional length was used to account for conduction through the cover plates to the fins. The conventional storage wall K/L reduces to the thermal conductivity of concrete divided by the thickness of the wall.

Interestingly, the thermal performance for varying aspect ratios and varying plate-fin thickness can be plotted on a single curve when plotted as a function of K/L . This result suggests that it is possible to determine the thermal performance of a transfer wall with a given fin spacing, plate-fin thickness, and plate-fin thermal conductivity, by calculating the total front-to-back surface conductance and interpolating the performance from Figures 7 and 8.

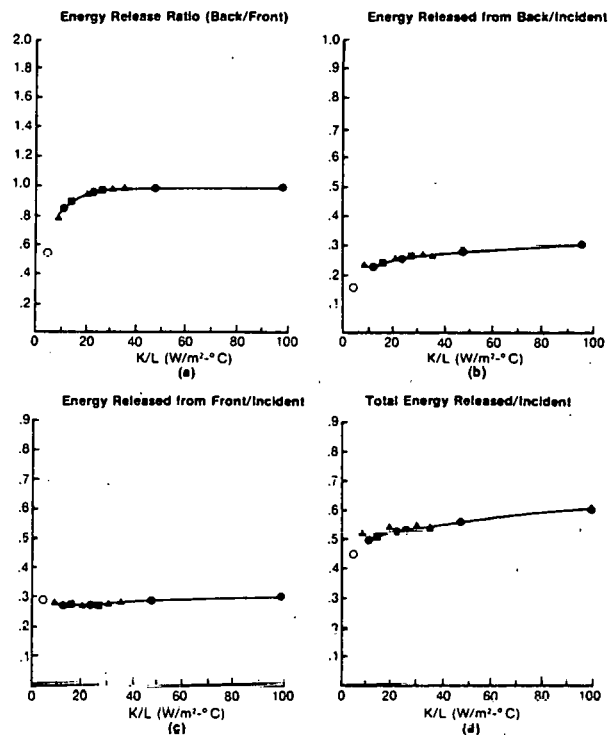


Fig. 8. The effect of aspect ratio and fin thickness during discharging. Aspect ratios of 4, 2, 1, and 0.5 and fin thicknesses of 2.54, 1.27, and 0.635 cm for an aspect ratio of 1 are shown, along with a conventional concrete storage wall (control). Also shown are results of various fin-plate thermal conductivities (triangles). Plate-fin materials used were stainless steel, iron, hydronalium, and silumin-copper with K/L values of 8.84, 20.62, 29.33, and 34.64, respectively. All values are integrated over the 18-hour discharging period.

The performance of transfer walls using other values for plate-fin thermal conductivity was determined, via simulation. The same charging and discharging scenario (6h and 18h, respectively) was used. Also, a constant aspect ratio (1.0) and constant plate-fin thickness (2.54 cm) were used. The total conductance, K/L , was varied by varying the thermal conductivity of the covering plates and connecting fins. The thermal conductivity of steel, iron, hydronalium, and silumin-copper (19, 72, 112, 137 $\text{W m}^{-1} \text{ } ^\circ\text{C}^{-1}$) were used in these simulations. The results (triangles) fall on the same curves plotted in Figures 7, 8, 9, and 10.

3.4 Selective ($\epsilon = 0.2$) Front Surface Coatings

The effect of a selective surface radiation coating applied to the front surface of the transfer wall is demonstrated in Figure 9 (charging) and Figure 10 (discharging). As in Figures 7 and 8, the thermal behavior of a transfer wall with and without a front selective surface coating, $\epsilon = 0.2$ and $\epsilon = 0.8$, respectively, are plotted against the total conductance K/L . The emissivity of the back surfaces is 0.8. In these simulations, the plate-fin thickness and thermal conductivity were constant, and the aspect ratio was varied to obtain different values for the total conductance (solid dots); or the aspect ratio was constant (1.0), and the plate-fin thickness (squares), or plate-fin thermal conductivity (triangles), was varied to obtain different values for the total conductance.

Charging. Figure 9a is the normalized energy gain (energy stored plus energy released from back surface) versus total conductance, K/L . Each point is the result from one storage wall. The normalized energy gain increases with the total conductance of the wall. The effect of a selective surface coating ($\epsilon = 0.2$) is to improve the gain by 8-14% over identical walls without a selective surface. A greater gain can be obtained from a transfer wall, $K/L = 20 \text{ W m}^{-2} \text{ }^\circ\text{C}^{-1}$, and a selective surface, as from a transfer wall with $K/L = 90 \text{ W m}^{-2} \text{ }^\circ\text{C}^{-1}$ and without a selective surface. This provides flexibility for cost trade-offs.

Figure 9b shows that almost all of the increase in energy gain from using a selective surface coating is stored. The reduction in energy released occurs at the front surface (Figure 9c). The amount of energy released from the back surface with and without selective surfaces is nearly identical (Figure 9d). Figure 9e demonstrates a large increase in the energy release ratio with increasing total conductance and with the use of a selective coating.

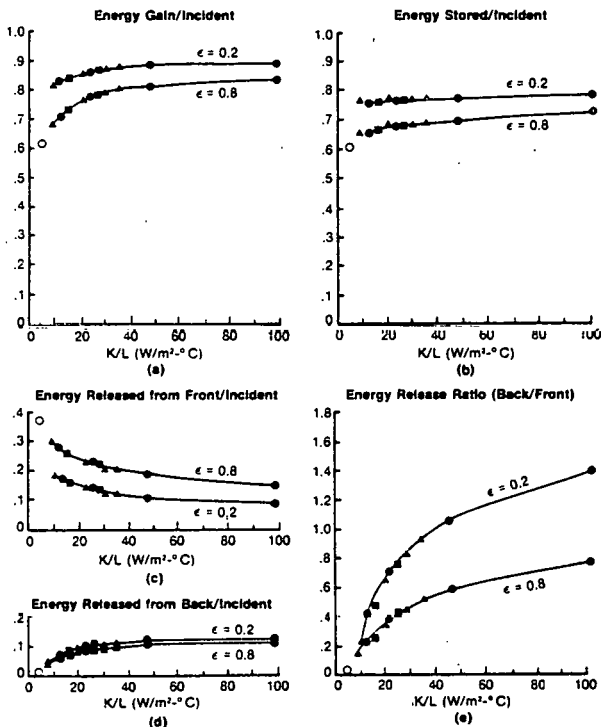


Fig. 9. Charging—The performance of transfer walls with a selective surface ($\epsilon = 0.2$) and without a selective surface ($\epsilon = 0.8$).

The effect of a selective surface coating is to store more energy during charging. Increased energy losses from the back surface during charging can only be achieved by increasing the total conductance from surface to surface. In this charging scenario, the energy released from the back surface approaches a constant at $K/L > 20 \text{ W m}^{-2} \text{ }^\circ\text{C}^{-1}$. More total conductance from front to back surface has little effect. The reason for this is that the small conductance from the surface to the sink node, via radiation and free convection, dominates the overall conductance from the front surface to the back sink node after $K/L > 20 \text{ W m}^{-2} \text{ }^\circ\text{C}^{-1}$.

Discharging. During discharging, the non-selective-surface ($\epsilon = 0.8$) energy release ratio increases with increasing total conductance, until a constant value of 1 is reached for $K/L > 20 \text{ W m}^{-2} \text{ }^\circ\text{C}^{-1}$. (Figure 10a). A selective coating on the front surface dramatically increases the energy release ratio for all transfer walls ($\epsilon = 0.2$). This increase reflects an increase in release from the back and a decrease in release from the front (Figures 10b and 10c). The total energy released is affected by an increase in total conductance and the use of a selective surface (Figure 10d).

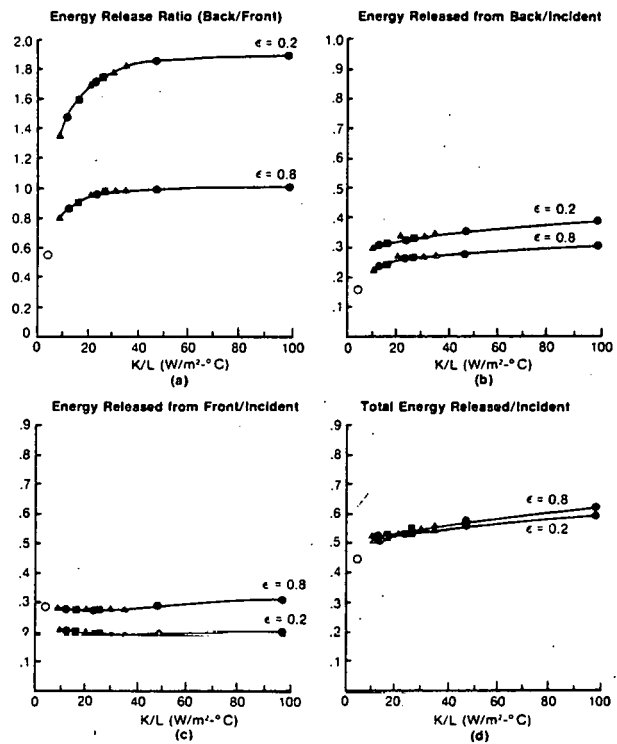


Fig. 10. Discharging—The performance of transfer walls with a selective surface ($\epsilon = 0.2$) and without a selective surface ($\epsilon = 0.8$).

4. SUMMARY AND DISCUSSION

4.1 Charging

Compared to a conventional storage wall, a substantial decrease, approximately 78%, in the amount of energy released from the front surface over a six-hour charging period can be achieved with an increase in total conductance and a selective surface. This is 30% of the total incident solar energy; it can be stored or released at the back surface. The amount stored increases with increasing total conductance.

The effect of a selective surface coating on the front surface is to increase the energy stored. An increase in energy released from the back surface is achieved by increasing the total conductance of the transfer wall. The increase in energy released from the back surface of a transfer wall over that of a conventional wall during charging is substantial, approximately 8 to 15 times, depending on the value of total conductance. In this test scenario, a constant value for the energy released from the back surface of approximately 10% of the incident energy is obtained at a value of $K/L > 20 \text{ W m}^{-2} \text{ }^\circ\text{C}^{-1}$. This value of 10% is not fixed because, in actual use, more energy will be transferred with increasing values of K/L as the back zone's load increases. Thus, if the temperature of this back zone (sink node) were $15.6 \text{ }^\circ\text{C}$ ($60 \text{ }^\circ\text{F}$), a larger percentage of the incident energy would be transferred and released from the back surface.

4.2 Discharging

The results demonstrate that a transfer wall with increasing values of K/L increases the amount of energy released from the back surface of the wall. Transfer walls with $K/L > 20 \text{ W m}^{-2} \text{ }^\circ\text{C}^{-1}$ discharge nearly equal amounts of energy from the front and back surfaces. Significantly more energy is discharged from the back surface when a selective coating is used on the front surface. This is an extremely advantageous characteristic for a storage wall in an indirect gain passive design.

4.3 Discussion

The described transfer wall exhibits many thermal characteristics that make it more desirable than a conventional concrete storage wall for direct gain multizone and indirect gain passive designs. By varying the total conductance (via aspect ratio, fin-plate thickness, and fin-plate thermal conductivity) and using a selective radiation coating, the improved performance of the transfer wall can be determined. This provides a degree of thermal control to the designer of a passive building.

Although a cost analysis has not been conducted, cost may be a potential drawback for the transfer wall. However, improved thermal control and performance, beyond that reported here, may be achieved when the transfer wall is combined with other systems presently being investigated, such as the "louver control system" (4). Together, the improved performance and control may justify additional costs. Also, ongoing investigations with water walls and other transfer wall designs may demonstrate that these walls can provide similar or better performance and/or control than this transfer wall, with minimal or no additional cost. Subsequent reports will discuss the results of these investigations and compare them to the transfer wall results presented in this paper.

5. REFERENCES

- 1 Conner, R. J., et al., "Martin Interactive Thermal Analysis System (MITAS)." MDS-SPLPD-71-FD238, June 1971, Martin Marietta Corporation, Denver, Colo.
- 2 Connolly, J. M., Bingham, C. E., and Ortega, J. K. E., "Computer Modeling of Thermal Storage Walls," TP-721-610, 1980, Solar Energy Research Institute, Golden, Colo. (To be presented at AS/ISES 1980 Annual Meeting).
- 3 Chapman, Alan J., Heat Transfer, 3rd ed., Macmillan, New York, 1974, p. 397.
- 4 Ortega, Joseph K. E., Holtz, Michael, Bingham, Carl, McDade, Mark, and Connolly, Michael, "Transparent and Opaque Louvers for Thermal Control in Passive Buildings," SERI/TP-721-611, 1980, Solar Energy Research Institute, Golden, Colo. (Submitted to the 5th National Passive Solar Conference, 1980).

Document Control Page	1. SERI Report No. TP-721-574	2. NTIS Accession No.	3. Recipient's Accession No.
4. Title and Subtitle Performance of Storage Walls with Highly Conductive Covering Plates and Connecting Fins		5. Publication Date May 1980	
7. Author(s) Joseph K. E. Ortega, Carl E. Bingham, J. Michael Connolly		6.	
9. Performing Organization Name and Address Solar Energy Research Institute 1617 Cole Boulevard Golden, Colorado 80401		8. Performing Organization Rept. No.	
		10. Project/Task/Work Unit No. 6321.10	
		11. Contract (C) or Grant (G) No. (C) (G)	
12. Sponsoring Organization Name and Address		13. Type of Report & Period Covered Technical Publication	
		14.	
15. Supplementary Notes			
16. Abstract (Limit: 200 words) The thermal behavior of a storage wall, constructed of concrete with highly conductive covering plates and connecting vertical fins, is investigated. The results demonstrate that, during the charging mode, the amount of energy released from the front surface is significantly reduced. A portion of the saved energy is stored for future discharge, but a large portion is transferred to the back surface and released. A selective front surface further reduces the energy released from the front surface, and this energy is stored. By properly selecting the fin spacing, plate-fin thickness, and plate-fin thermal conductivity, the rate and direction of thermal discharge can be controlled. The improved heat transfer capability and added thermal control provide new alternatives for interzonal heat transfer and multizone passive building designs.			
17. Document Analysis a. Descriptors Thermal Storage Walls; Trombe Walls; Passive Solar Heating; Charging Mode; Discharging Mode; Fin Spacings; Conductance; Coverings b. Identifiers/Open-Ended Terms c. UC Categories 59			
18. Availability Statement National Technical Information Service U. S. Department of Commerce 5285 Port Royal Road Springfield, Virginia 22161		19. No. of Pages 5	
		20. Price \$4.00	